A PHYSICALLY-BASED SMALL-SIGNAL CIRCUIT MODEL FOR HETEROSTRUCTURE ACOUSTIC CHARGE TRANSPORT DEVICES

J. Stevenson Kenney and William D. Hunt, School of Electrical Engineering and Microelectronics Research Center, 777 Atlantic St. NW, Georgia Institute of Technology, Atlanta, GA 30332-0250

Abstract—**This paper presents a small-signal circuit model for heterostructure acoustic charge transport (HACT) devices. Circuit elements and noise sources are derived from operating conditions and physical device parameters. Frequency response and noise figure are simulated using Libra™. They agree within 1 dB of measured data.**

1. INTRODUCTION

Acoustic charge transport (ACT) devices are charge transfer devices similar in operation to charge-coupled devices (CCDs). Both ACTs and CCDs transfer charge confined in moving potential wells. CCDs rely on an array of differently phased clock potentials to move the charge along the channel. In contrast, ACTs rely on a potential induced in a piezoelectric semiconductor, such as GaAs, by a surface acoustic wave (SAW). In this way, they eliminate the complicated air-bridged network of gate electrodes. The first ACT devices demonstrated relied on surface and back-gating potentials to confine the charge within the channel. More advanced devices have been recently demonstrated which use the band-gap potential between an AlGaAs and a GaAs layer to confine the charge [1]. Such devices, shown schematically in Figure 1, have hence been called *heterostructure acoustic charge transport* (HACT) devices. The basic architecture of many HACT devices is that of a periodically tapped transversal filter, similar to those realized using digital signal processing (DSP) techniques. Being parallel analog processors, HACT devices offer a three-order of magnitude improvement in speed (bandwidth) over DSP-based transversal filters. Because of this, they have found applications as high-speed equalizers, programmable filters, and correlators [2]. Given these increasingly complex applications, computer modelling of HACT devices has become important not only to device designers, but also to systems designers who wish to predict overall performance based on device performance. In view of this, a device model must be detailed enough so that adequate information concerning device geometry and material parameters can be incorporated. It must also be flexible enough to provide tractable system level performance predictions. Previously reported models fall into two categories which address these needs individually. Computationally intensive Poisson-based physical models [3], [4] provide information about the charge density and potential within the device, but dynamic terminal characteristics are not easily obtained. Empirically based behavioral models [5], [2] provide adequate information for the system designer, but do not relate this to the internal operation of the device. We present a compromise between these two types with a physically-based small-signal circuit model. The element values of this model are derived from the device physics. The model can also be easily implemented on commercially available microwave circuit analysis software.

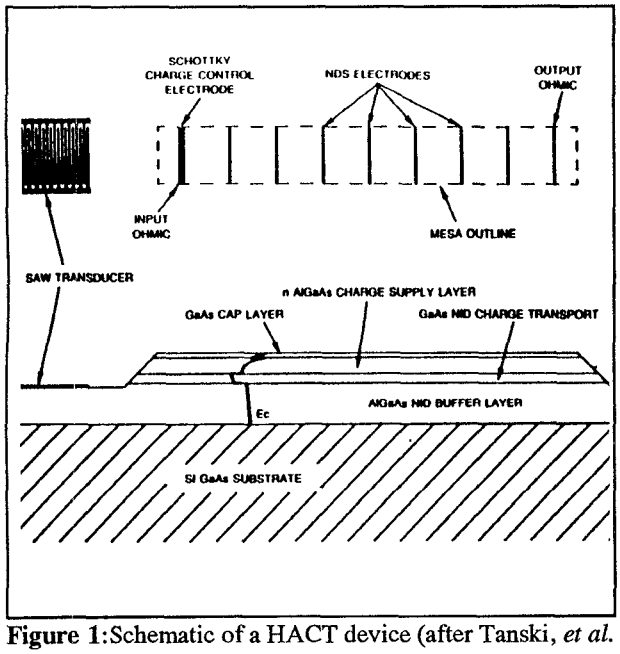

Figure 1: Schematic of a HACT device (after Tanski, *et al.* [1]).

The circuit model is divided into three sections which are related to the operational functions of the device: input sampling (charge injection), charge transport, and output sensing. This paper will concentrate on a physical model for the charge injection process. Charge transfer and sensing are covered in detail in the authors' previous paper [6], and we will present only the results in this paper. With the development of the new charge injection model, the existence of shot noise has been proven, and hence will be covered in detail. Other noise sources were treated in [6], and will be summarized here.

VV

CH3277-1/93/0000-1513$01.00 © 1993 IEEE

2. INPUT CIRCUIT

The operation of the input circuit consists of a conversion of voltage to charge, and the subsequent removal of charge by the transport process. The input structure resembles a HEMT, and as such, is modelled by a nonlinear voltage controlled current source. Differences between the two devices become apparent when one considers the channel potential. Under normal operation all charge is moved by the SAW potential travelling at the acoustic velocity, which is roughly two orders of magnitude slower than the saturation velocity of GaAs. The epitaxial layers are also different from those used for HEMT devices. The AlGaAs charge control layer is more lightly doped, and the GaAs cap layer is left undoped so as not to "short out" the SAW potential at the surface. A third difference is that HACT devices are operated with the channel completely pinched off. In this mode, the only current that flows in the channel is that due to the *subthreshold* effect [7]. In a conventional MESFET operating in this regime, charge present in the n^+ ohmic region diffuses over the potential barrier set up by the gate voltage. Thus the operation is similar to a bipolar transistor, and the channel current is an exponential function of gate voltage V_{GS}. Following Liang *et al.*, we develop the HACT injection model by considering the SAW potential at the transport channel *Vc* to be superimposed on the gate, depletion, and conduction band potentials. A surface charge potential also exists in GaAs devices [1]. Considering this, and assuming that the charge concentration in the channel is always much less than that in the ohmic source region, an expression for the instantaneous channel current $I_c(V_{gs}, V_c)$ can be developed.

$$I_c(V_{GS}, V_c) = \frac{WqD_n n_{eff}}{L_G} e^{\frac{q}{\eta kT}(V_{GS} - V_{th} + V_c(x=0,t))} \quad (1)$$

where W is the channel width, q is the elementary charge, D_n is the diffusion coefficient, n_{eff} is the effective doping in the source region, L_G is the gate length, η is the ideality factor, k is Boltzmann's constant, T is the absolute temperature, V_{th} is the threshold voltage for a HEMT [8]. The average channel current $\langle I_c(V_{GS})\rangle$ for a sinusoidally varying channel potential of amplitude ϕ_s can be obtained by integrating Eq. (1) over one SAW period T_s. This can be done analytically in approximate form by expanding out the channel to get a Gaussian function in the integrand. Expanding the limits of integration to infinity yields little error, so that the definite integral can be solved to obtain

$$\langle I_c(V_{GS})\rangle \approx \frac{WqD_n n_{eff}}{L_G}\sqrt{\frac{\eta kT}{2\pi q\phi_s}} e^{\frac{q}{\eta kT}(V_{GS} - V_{th} + \phi_s)} \quad (2)$$

A plot of Eq. (2) is shown below in Figure 2, along with the measured $\langle I_c\rangle$-V_{GS} curve of a 1 mm wide HACT device.

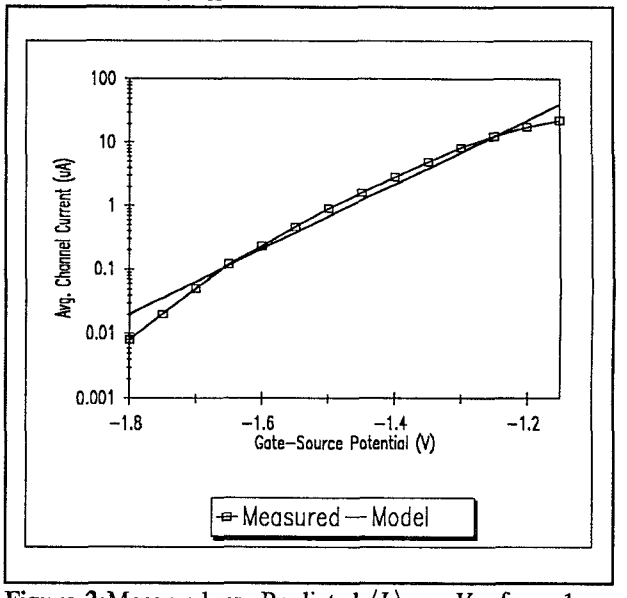

Figure 2:Measured vs. Predicted $\langle I_c\rangle$ vs. V_{GS} for a 1mm HACT device. η = 3.3, ϕ_s = 0.26 V.

The small-signal average transconductance $\langle g_m\rangle$ about some operating point V_{GS0} is obtained by differentiating Eq. (2).

$$\langle g_m\rangle = \frac{WqD_n n_{eff}}{L_G}\sqrt{\frac{q}{2\pi\phi_s\eta kT}} e^{\frac{q}{\eta kT}(V_{GS0} - V_{th} + \phi_s)} \quad (3)$$

An expression for the total charge injected into the mth packet Q_m was derived in [6]

$$Q_m = Q_0 + T_s\langle g_m\rangle\langle v_{gs}\rangle_m \equiv Q_0 + c_s\langle v_{gs}\rangle_m = Q_0 + q_m \quad (4)$$

where $Q_0 = T_s\langle I_c(V_{GS0})\rangle$. We have defined a linear small-signal conversion capacitance c_s which relates the sampled small-signal voltage $\langle v_{gs}\rangle_m$ to the signal charge packet q_m. Thus it is equivalent to model the injection process with either a time-averaged transconductance, or a two-port capacitance. The former is more conventional, and is shown in small-signal model for the input injection process in Figure 3. The effect of averaging over the aperture width in the sampling is a rolloff in the frequency response [2]. We have found this rolloff to be negligible below the Nyquist frequency. Thus $\langle v_{gs}\rangle_m \approx v_{gs}(t - mT_s)$, and the circuit is completely linear.

Parasitic elements are also present in the input circuit. These are essentially the same as those of a GaAsFET of comparable geometry and material characteristics. Physically-based expressions are given in [9].

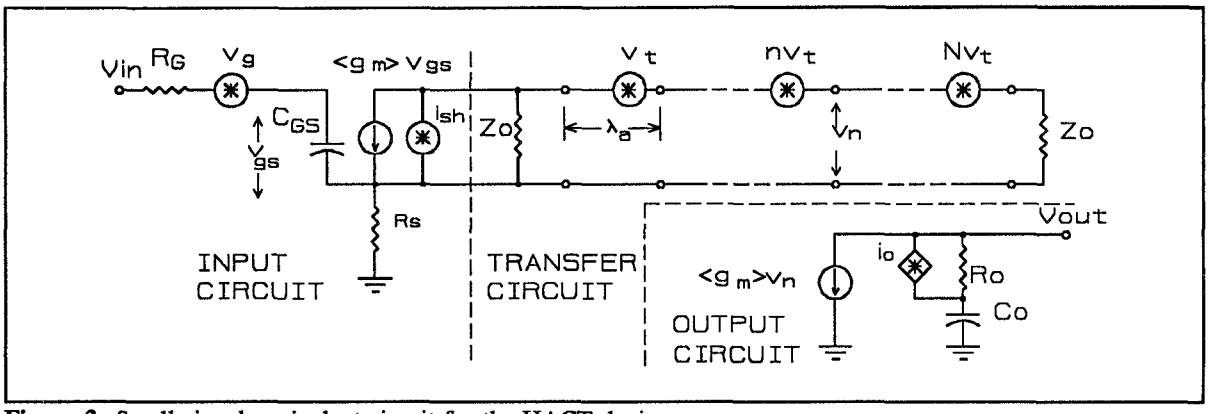

Figure 3: Small-signal equivalent circuit for the HACT device

3. TRANSFER CIRCUIT

Once the charge packets have been injected into the transport channel, they are transferred continuously at the acoustic velocity. Since the small-signal charge is linearly related to the small-signal voltage by the effective storage capacitance c_s, we can treat the charge packet as an equivalent voltage propagating on an ideal unidirectional transmission line, as shown in Figure 3. The impedance of the line is determined uniquely by the shunt capacitance per unit length C, and the acoustic velocity V_a. Since the we require the charge packet q_m associated with the equivalent potential v_{gs} to be related by the storage capacitance, the capacitance per unit length is simply c_s/λ_a. The equivalent series inductance per wavelength is found from

$$V_a = \frac{1}{\sqrt{LC}} \Rightarrow L = \frac{\lambda_a}{V_a^2 c_s} \tag{5}$$

4. OUTPUT CIRCUIT

The NDS elements are essentially reversed biased Schottky diodes. The charge packets are capacitively coupled to the output electrodes. They induce a positive image charge on the NDS elements, each having a capacitance C_O. Because the charge is confined close to the surface, the image charge on the NDS electrodes is essentially equal to the channel charge [11]. The Norton equivalent circuit is most convenient to model the NDS tap as multiple taps can simply be current summed.

$$\langle i_o \rangle_n \approx \frac{q_m}{T_s} = \frac{c_s}{T_s}\langle v_{gs} \rangle_{m+n} = \langle g_m \rangle \langle v_{gs} \rangle_{m+n} \tag{6}$$

A parasitic resistance R_O appears in series with C_O as shown in Figure 3. The value of these must usually be determined empirically, although some estimates can be made with material parameters and geometry.

5. NOISE SOURCES

Noise arises from several random processes within the HACT device. The dominant source of noise at the input is due to the *thermal noise* of the gate and source resistances R_G and R_S. Since the gate capacitance C_{GS} is ordinarily very small, the rolloff of the noise power occurs at frequencies substantially higher than the Nyquist frequency. For this reason, the input noise voltage (amplitude squared) per unit bandwidth $|v_g|^2$ can be considered constant.

$$|v_g|^2 = 4kT(R_G + R_S) \tag{7}$$

where k is Boltzmann's constant and T is the absolute temperature.

There is also thermal noise associated with the output resistance R_O, which can contribute to the total output noise for low gain devices. It appears as a noise current source in parallel with R_o as shown in Figure 3. The noise current (amplitude squared) is given by

$$|i_o|^2 = \frac{4kT}{R_o} \tag{8}$$

Because the charge injection is a barrier-limited process, *shot noise* is also present in the channel current. The mean-square amplitude per unit bandwidth is related to the steady-state channel current.

$$|i_{sh}|^2 = 2q\langle I_c(V_{GS0}) \rangle \tag{9}$$

Transfer noise mainly arises from the random trapping and emission of carriers in GaAs/AlGaAs interface and bulk impurity states [6]. The noise power spectral density of this type of noise is difficult to calculate because of the correlation between fluctuations in adjacent packets. We consider the total fluctuation to be band limited by the sampling frequency. This is justified since only interface

states with time constants of the order of a SAW period contribute to the transfer noise. Thus, the equivalent input voltage $|v_t|^2$ is

$$|v_t|^2 = \frac{\alpha kTqn_t AT_s}{c_s^2} \qquad (10)$$

where A is the charge packet area and α is a constant determined by trap energy and cross section energy distribution. A typical value cited in the CCD literature for uniform energy distribution is $\alpha = 2 \cdot ln(2)$ [6].

6. CIRCUIT SIMULATION

Figure 4 shows the results of a frequency response and noise figure simulation of a 160 tap, 144 MHz HACT device implemented on Libra™, a commercially available microwave analysis program [10]. The measured response is also shown for comparison. The transconductance was determined by Eq. (3). The input and output parasitics, R_G, R_S, C_{GS}, R_O, C_O were determined by measurement. The average error above -30 dB insertion loss was less than 1.0 dB. Below this level, the frequency response is adversely affected by measurement noise and slight deviation from ideal tap weights within the device. Thermal noise models are inherent in the element definitions of resistors in Libra™. Noise sources were added to simulate the shot noise (Eq. (9) and transfer noise (Eq. (10). The predicted noise figure at band center is less than 0.5 dB from that measured using the y-factor method.

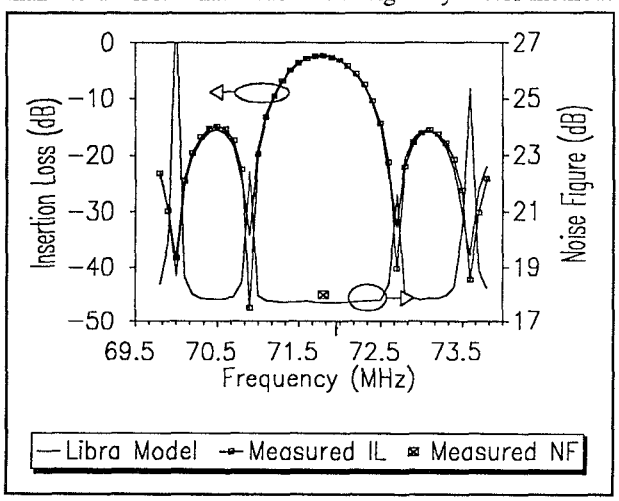

Figure 4: Measured and simulated small-signal gain of a 160 tap HACT device.

7. SUMMARY AND CONCLUSIONS

The purpose of this paper was to relate the small-signal operation of HACT devices to the physical geometries, material parameters, and operating conditions of the device. We developed a model of charge injection based on subthreshold current in GaAsFETs. Good agreement was obtained between measured and predicted $\langle I_c \rangle$-V_{GS} curves. The model was then applied to a linear model developed previously by the authors to study gain and noise figure. This was implemented on Libra™, and gain and noise figure were predicted for a 160 tap HACT device. The predicted gain was less than 1 dB from the measured data (above -30 dB insertion loss). The predicted midband noise figure was within 0.5 dB of the measured NF.

BIBLIOGRAPHY

[1] W.J. Tanski, S.W. Merrit, R.N. Sacks, and D.E. Cullen, "Heterojunction Acoustic Charge Transport Devices on GaAs," *Appl. Phys. Lett.*, Vol. 52, No. 1, pp. 18-19, Jan. 4, 1988.

[2] R.L. Miller, C.E. Nothwick, and D.S. Bailey, *Acoustic Charge Transport Devices*, Boston: Artech House, 1992.

[3] E.G. Bogus, "Electrical Charge Injection in an Acoustic Charge Transport Device," Ph. D. Dissertation, University of Illinois, Champaign, IL, 1987.

[4] G.A. Peterson, B.J. McCartin, W.J. Tanski, and R.E. LaBarr, "Charge Confinement in Heterojunction Acoustic Charge Transport Devices," *Appl. Phys. Lett.*, Vol. 55, No. 13, pp. 1330-32,,Sept. 25, 1989.

[5] S.W. Merrit, "Heterostructure Acoustic Charge Transport Device Model," *Proc. 1990 Ultrasonics Symp.*, pp. 247-252, Dec. 4-7, 1990.

[6] J.S. Kenney and W.D. Hunt, "A Small-Signal Equivalent Circuit Model for Heterostructure Acoustic Charge Transfer Devices," *Proc. 1992 Ultrasonics Symp.*,. Oct. 20-23, 1992.

[7] C.L. Liang, N.W. Cheung, R.N. Sato, M. Sokolich, and N.A. Doudoumopoulos, "A Diffusion Model of Subthreshold Current for GaAs MESFETs," *Solid-State Electron.*, Vol. 34, No. 2., pp131-38, 1991.

[8] J.M. Golio, ed. *Microwave MESFETs and HEMTs*, Boston: Artech House, 1991.

[9] R. Williams, *Modern GaAs Processing Techniques*, Boston: Artech House, 1990.

[10] *Libra* is available from EESof, Inc., 5601 Lindero Canyon Rd., Westlake Village, CA 91362.

[11] C.E. Warren, *Nondestructive Sensing in Buried Channel Travelling Wave Charge Transfer Devices*, M.S. Thesis, University of Illinois, 1984.

ACKNOWLEDGEMENT

We wish to thank Don Cullen of United Technologies Research Center, for supplying HACT devices to us for research purposes.